

Multiple capture locations for 3D ultrasound-guided robotic retrieval of moving bodies from a beating heart

Paul Thienphrapa^{a,b}, Bharat Ramachandran^a, Haytham Elhawary^a,
Russell H. Taylor^b, Aleksandra Popovic^a

^aPhilips Research North America, 345 Scarborough Rd., Briarcliff Manor, NY 10510, USA;

^bJohns Hopkins Univ., ERC CISST/LCSR, 3400 N. Charles St., Baltimore, MD 21218, USA

ABSTRACT

Free moving bodies in the heart pose a serious health risk as they may be released in the arteries causing blood flow disruption. These bodies may be the result of various medical conditions and trauma. The conventional approach to removing these objects involves open surgery with sternotomy, the use of cardiopulmonary bypass, and a wide resection of the heart muscle. We advocate a minimally invasive surgical approach using a flexible robotic end effector guided by 3D transesophageal echocardiography. In a phantom study, we track a moving body in a beating heart using a modified normalized cross-correlation method, with mean RMS errors of 2.3 mm. We previously found the foreign body motion to be fast and abrupt, rendering infeasible a retrieval method based on direct tracking. We proposed a strategy based on guiding a robot to the most spatially probable location of the fragment and securing it upon its reentry to said location.

To improve efficacy in the context of a robotic retrieval system, we extend this approach by exploring *multiple candidate capture locations*. Salient locations are identified based on spatial probability, dwell time, and visit frequency; secondary locations are also examined. Aggregate results indicate that the location of highest spatial probability (50% occupancy) is distinct from the longest-dwelled location (0.84 seconds). Such metrics are vital in informing the design of a retrieval system and capture strategies, and they can be computed intraoperatively to select the best capture location based on constraints such as workspace, time, and device manipulability. Given the complex nature of fragment motion, the ability to analyze multiple capture locations is a desirable capability in an interventional system.

Keywords: 3D ultrasound guidance, 3D TEE-based tracking, medical robotics, beating heart, foreign bodies

1. INTRODUCTION

Penetration of a foreign body into the heart is a common injury in both civilian accidents and military warfare.^{1,2} It can occur as a result of embolization from the venous vasculature after a soft tissue injury in the chest, abdomen, or extremities. This usually results in a foreign body being lodged in the pericardial wall. However, small caliber bullets and small shell fragments with low velocity tend to circulate freely in the chambers, typically the right atrium, and can become entrapped in the pericardial trabeculations and fatty tissue.³ The condition has the potential to cause arrhythmia, occlusion, and death.^{3,4}

1.1 Conventional treatment

A direct injury is usually accompanied with severe life-threatening symptoms such as hemorrhage and cardiac tamponade, requiring a fast response to stabilize the patient.¹ Once the patient is stabilized, cardiac surgery is performed to remove foreign objects and, if needed, repair the pericardium. Embolized foreign bodies can be symptomatic or asymptomatic.⁵ Symptomatic, free-moving foreign bodies usually cause the conditions mentioned above and have to be removed surgically. Localization of foreign objects is commonly performed using chest X-ray or ultrasound imaging.² Due to the difficulty of manipulating catheters to retrieve moving targets, the most frequent treatment approach is a median sternotomy, followed by an incision in the pericardium to expose the heart chamber and the object.^{1,5-7} (Left/right thoracotomy is an alternative approach.) Median

Correspondence: Paul Thienphrapa

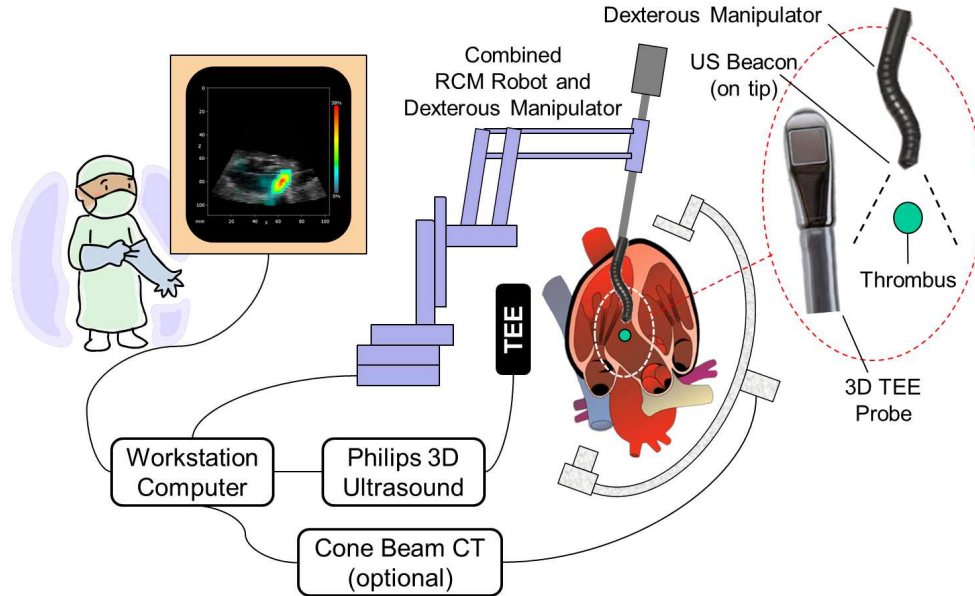


Figure 1. Robotic fragment retrieval from the heart under 3D TEE guidance.

sternotomy is a highly invasive procedure requiring a long recovery period, and incurs numerous risks including bacterial mediastinitis, inflammation, and bone fracture. Moreover, patients risk future injury if undergoing cardiopulmonary resuscitation (CPR) due to the sternotomy wires and staples.⁸ A standard setting may employ cardiopulmonary bypass (CPB), which is associated with risks of hemolysis, clotting, and air embolism.

1.2 Purpose of study

Minimally invasive retrieval of a moving body from a beating heart using 3D transesophageal echocardiography (TEE) and a flexible robotic end effector can help avoid the perioperative and postoperative risks associated with sternotomy and CPB. It is, however, a technically challenging endeavor due in large part to the relatively irregular motion of the fragment. In the envisioned surgical procedure, a robotic tool is inserted transapically into the heart (Fig. 1) after identification of the foreign body under preoperative imaging. Then under intraoperative ultrasound guidance, the robot moves to capture the target; the end effector should be flexible for adequate workspace coverage. The purposes of the current effort include (1) the establishment of an experimental platform for real-time, 3D TEE-based tracking and robot guidance to serve as a basis for a minimally invasive surgical system; (2) the acquisition and analysis of experimental data to improve understanding of the problem from clinical and technical perspectives, aid in system development, and illuminate potential solutions; and (3) the assessment of proposed solutions.

2. RELATED WORK

The use of 3D ultrasound for surgical robot guidance continues to be an emerging development due to cost, low resolution, and inability to access real-time data streams.⁹ Early experiments using 3D transthoracic echocardiography (TTE) featured ultrasound-based instrument tracking using markers attached to the tool.¹⁰ The tracking error was less than 1 mm, with a robot speed of 3 mm/s and an algorithm update rate of 2 Hz. In subsequent water tank experiments, the instrument was guided towards static physical (i.e. non-virtual) targets with an error of 1.2 mm.¹¹ Compact 3D catheter transducers have been shown to perform with errors of around 3 mm.¹²

Increased robotic performance was seen in one-degree-of-freedom (DOF) handheld heartbeat compensation devices designed for beating heart mitral valve repair; errors were on the order of 1 mm based on water tank experiments.^{13,14} Ferrous shrapnel, resting against a hyperechoic background, can be illuminated under color flow Doppler using a variable magnetic field. Such targets can be located within an RMS error of 1.06 mm.¹⁵ The approach bears similarity to work using piezoelectric buzzers to induce vibrations in a surgical tool.¹⁶

There are key distinctions between the aforementioned achievements and the current effort. First, the previous works^{10–12,17} experiment with static targets in a water tank, while the target in the foreign body retrieval procedure moves abruptly and in a dynamic environment. Additionally, predominantly 1-DOF periodic mitral valve motion is particularly amenable to predictive tracking to overcome processing delays (8 Hz update), but a predictive control scheme is less likely to be effective on a cardiac foreign body, which is prone to seemingly arbitrary motions.¹⁸ Our efforts focus on tracking of an unpredictable target using 3D TEE.

Outcomes of a precursor study that we reported in Ref. 18 include: (1) tracking of a foreign body in a beating heart phantom using 3D TEE; (2) characterization of foreign body motion; and (3) proposition of indirect foreign body retrieval strategies. We quantified, in particular, a method using the spatial probability of fragment location. These findings (Table 1) motivate the exploration of different indirect retrieval concepts. This paper expands upon our preliminary examination by considering additional approaches of interest (Sec. 4.1), seeking new perspectives on retrieval strategies for a flexible, minimally invasive robotic device.

Table 1. Summarized results of previous experiments.¹⁸

Tracking		Motion Characteristics			Indirect Retrieval	
RMS Error	2.3 mm	Range	40.2 mm		Spatial Probability	50.5%
		Speed	343.5 mm/s			
		Acceleration	7800.0 mm/s ²			

3. MATERIALS AND METHODS

As this effort builds upon our previous work, details of the materials and methods used can be found in previous reports;¹⁸ the descriptions are partially reproduced here for clarity.

3.1 Experimental setup

A system for studying the problem of minimally invasive evacuation of fragments from a beating heart is illustrated in Fig. 2 (*left*). The experimental setup consists of an ultrasound system (Philips iE33 xMATRIX Echocardiography System with Philips X7-2t 3D TEE probe), a beating heart phantom (a replica of a human heart made of polyvinyl alcohol cryogel) in a water tank, and a workstation (2.3 GHz Intel Xeon, 4 GB of RAM) for acquiring streaming ultrasound volumes over TCP/IP. Servo-actuated pneumatic pistons pump water into and out of the heart phantom to create the deformable effect of a heartbeat and blood flow. The motion of the pistons, plotted in Fig. 2 (*right*), is programmed with a heart rate of 1 Hz and stroke volume of 18 ml to mimic conditions during surgery.¹⁹ The ultrasound image frames have a resolution of $128 \times 48 \times 112$ voxels of size 0.81, 0.96, and 0.98 mm, spanning a field of view of 60° azimuth, 30° elevation, and 12 cm depth respectively. Gain and compression are set to 47% and 40 dB.

As an approximation, a 3.2-mm steel ball was inserted into the right ventricle of the heart phantom to act as a fragment due to its similarity to a clinical trauma case in terms of size (typically 2-5 mm) and material. The fragment was imaged under 3D TEE at 20 frames per second (fps) and manually segmented from five datasets ($n = 5$) of 400 frames (20 seconds) each. This duration was empirically found to capture most of the activity that would occur in a given trial. Furthermore, 20 heart cycles permit robust testing of online tracking methods—a previous study reports on an *in vivo* instrument tracking experiment using a five-second window.²⁰ Fig. 3 shows the fragment in the heart phantom manually outlined in the 3D TEE image.

3.2 Fragment tracking

To achieve real-time tracking of the fragment,¹⁸ we use normalized cross-correlation (NCC), a well-known algorithm used for matching a template $t(x, y, z)$ against a subimage $f(x, y, z)$. Normalization provides for tracking robustness against changes in intensity, which can occur as both the fragment and background move. The basic

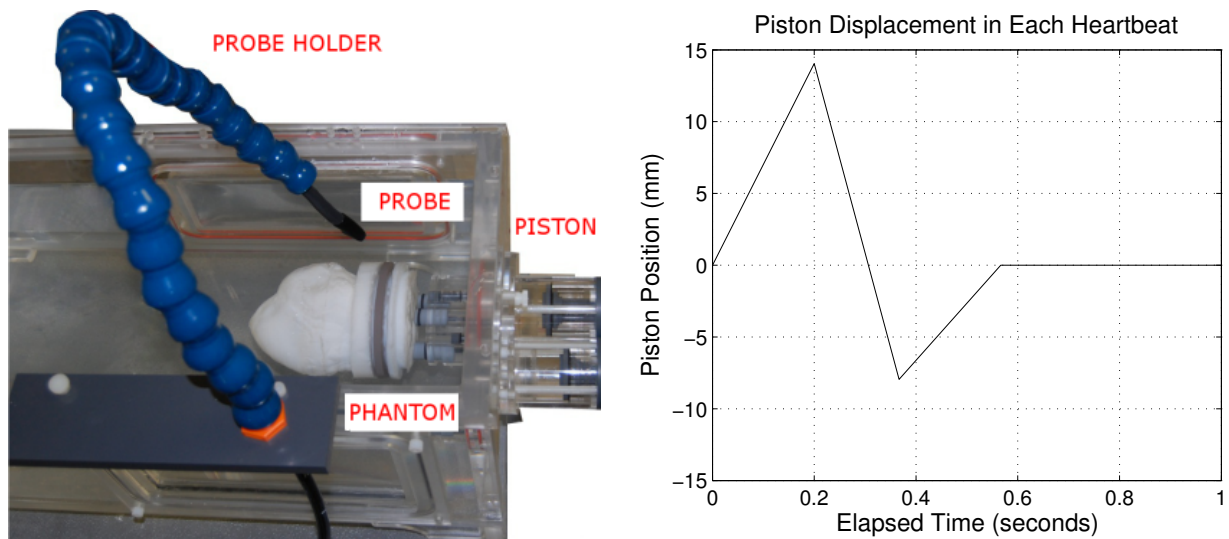


Figure 2. (Left) Arrangement of the TEE probe and the heart phantom. (Right) Piston displacement in the beating heart phantom for one heartbeat.

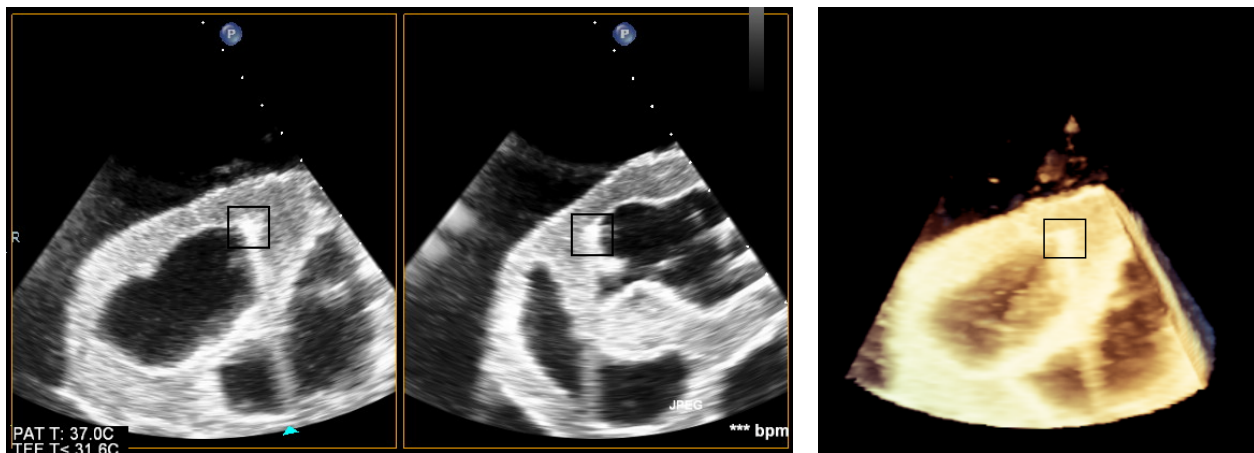


Figure 3. (Left and Center) Orthogonal slices showing the fragment (outlined) in the right ventricle of the heart phantom at rest. (Right) A three-dimensional view.

form of NCC is given in Equation (1); a detailed description of the technique can be found in standard image processing texts.²¹

$$R(u, v, w) = \frac{\sum_{x,y,z} [f(x, y, z) - \bar{f}] [t(x - u, y - v, z - w) - \bar{t}]}{\sqrt{\sum_{x,y,z} [f(x, y, z) - \bar{f}]^2 \sum_{x,y,z} [t(x - u, y - v, z - w) - \bar{t}]^2}} \quad (1)$$

The fragment is selected interactively from the first image frame to define the template for the algorithm to track in subsequent frames. A template of size $10 \times 10 \times 10$ voxels is suitable for enclosing the entire fragment, while a search space of $40 \times 30 \times 30$ is sufficient to capture displacements between frames. The fast computation time of NCC (38 ms per frame) makes it especially suitable for tracking when real-time performance is required.

The coefficient R in the equation above is a real number in $[-1, 1]$, with higher values indicating a close match. The location of the maximum R (R_{max}) per frame is taken to be the position of the fragment. NCC is not very robust to the noise, artifacts, and low resolution inherent in ultrasound images, but we previously found that by skipping frames in which $R_{max} < R_{mean} - c \cdot R_{stddev}$ (suggesting that the algorithm was not confident in its decision), errant tracking can be avoided and an RMS error of 2.3 mm can be achieved after dropping 18.5% of frames.¹⁸ This approach is advantageous for the current study due to its simple implementation, while yielding acceptable spatial and temporal performance. The fragment motion was found to be fast and seemingly arbitrary, necessitating indirect retrieval strategies. Frequency domain analyses in accord with that of the mitral valve¹³ support this conclusion as well.

4. EXPERIMENTS

4.1 Candidate capture locations

Given the difficulty and risk in robotically chasing a foreign body in a beating heart, as well as its preference towards certain positions and paths, the goal then is to optimally position the end effector for a successful intercept. Previously, the best candidate capture location (CCL) was implicitly defined as that with the highest spatial probability of containing the foreign body. In this work we generalize the concept, identifying several candidates from which an interventional system may select based on various criteria. The types of candidates are described below, and their measured results are listed in Table 2.

- *Maximum occupation time (spatial probability)*: Which locations are expected to contain the fragment the most? This metric may be applicable to a slower end effector with a capture mechanism that activates relatively quickly, such as a gripper.
- *Maximum dwell time*: How long does the fragment dwell in a certain location before it leaves (t_{dwell})? When it leaves, how long does the system have to wait before the fragment reenters said location (t_{wait})? These metrics may be useful for capture mechanisms that are slower to activate, such as suction.
- *Maximum visit frequency*: How often does the fragment visit, or traverse, a certain location? This metric may be suitable for a mechanism such as a net that best captures a fragment in transit.

The overall average values (mean column of Table 2) can be used to inform the design of a robotic system and retrieval strategy. The most occupied location contains the target 50.5% of the time, the longest dwelled location contains it for 0.84 s (with 2.28-s gaps), and the most frequently visited location sees it 1.54 times per second. We note the inter- and intra-dataset variances, concluding that online estimates must be used. In the envisioned operation, the system observes the fragment motion and computes the optimal capture location in real time, based on criteria such as reachability, time to execute trajectory and capture, and obstacles detected via preoperative and intraoperative sensing. The robot is then guided to said location to secure the fragment upon its reentry. The relative importance of these criteria are to be determined in future work. The distances between candidates, depicted in Fig. 4 and in the last three rows of Table 2, confirm that the candidate capture locations are indeed distinct locations.

Table 2. Measurements of candidate capture locations.

Parameter	Datasets					Aggregate			
	A	B	C	D	E	Min	Mean	Max	SD
<i>CCLA</i> : % time occupied by moving body in most occupied location									
% Time ¹⁸	39.8	38.0	57.5	54.0	63.0	38.0	50.5	63.0	11.1
<i>CCLB</i> : Dwell and wait times in longest-dwelled location									
Avg. t_{dwell} (s)	0.33	0.54	2.00	0.49	0.85	0.33	0.84	2.00	0.83
Avg. t_{wait} (s)	3.58	1.75	1.59	3.40	1.07	1.07	2.28	3.58	3.55
<i>CCLC</i> : Frequency of visits to most frequently visited location									
Visits/s	1.25	0.95	1.70	2.00	1.80	0.95	1.54	2.00	0.43
Distances between candidate locations									
$ CCLA - CCLB $ (mm)	10.77	5.96	5.47	6.74	6.55	5.47	7.10	10.77	2.11
$ CCLB - CCLC $ (mm)	12.87	4.35	4.38	7.43	4.65	4.35	6.74	12.87	3.66
$ CCLC - CCLA $ (mm)	4.07	2.70	2.12	1.26	2.13	1.26	2.46	4.07	1.04

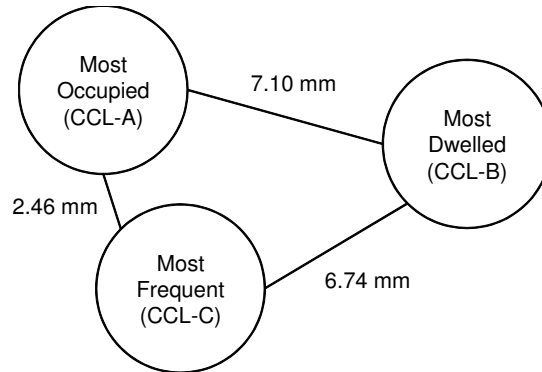


Figure 4. Diagram illustrating that candidate capture locations (CCLs) are distinct. An interventional system can make selections based on workspace and robot constraints.

4.2 Capture range

The type of retrieval mechanism ultimately deployed will determine the degree of accuracy necessary to successfully capture the moving body. Certain mechanisms may have larger functional ranges than others, as illustrated in Fig. 5. Equivalently, certain mechanisms may tolerate larger positioning errors than others. In this section, we examine the effect that the inherent *capture range* of a device may have on computation of the various candidate capture locations. As an estimate, we model the operative volume of the end effector as a binary sphere, wherein the foreign body is successfully captured if it falls within it. We are interested in being able to predict the performance of our methods for devices of different capture ranges (nominally 5 mm).

Fig. 6 shows that capture location measurements improve with increasing capture range, as expected. From a design perspective, one observation is the saturation of performance above a 7 mm range in many cases. Dwell time (center plot of Fig. 6) is computed as an average over the capture range and thus appears to decrease above 7 mm. When instead computed as a maximum, the expected monotonic increase is restored, as shown in Fig. 7. The average view is presented first, as maximum values are more sensitive to per-trial variabilities.

Noticeable deviations from the average behavior suggest that the motion can fall into different, possibly aperiodic, modes. It is thus advisable to augment the aforementioned calculations by recording secondary locations (e.g. second-highest occupation time) to increase the number of candidates, and by retaining sliding-window histories to adapt to slow, aperiodic changes in fragment behavior.

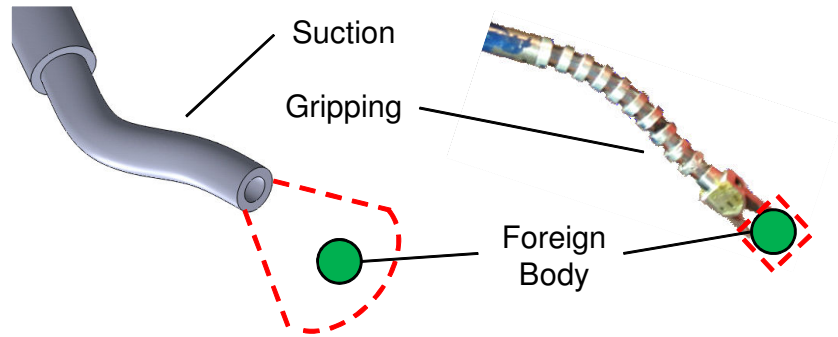


Figure 5. Example of two potential capture mechanisms, suction (*left*) and gripping (*right*), with different inherent capture ranges indicated by dashed lines. Suction may tolerate greater positioning error, but a gripper may activate faster.

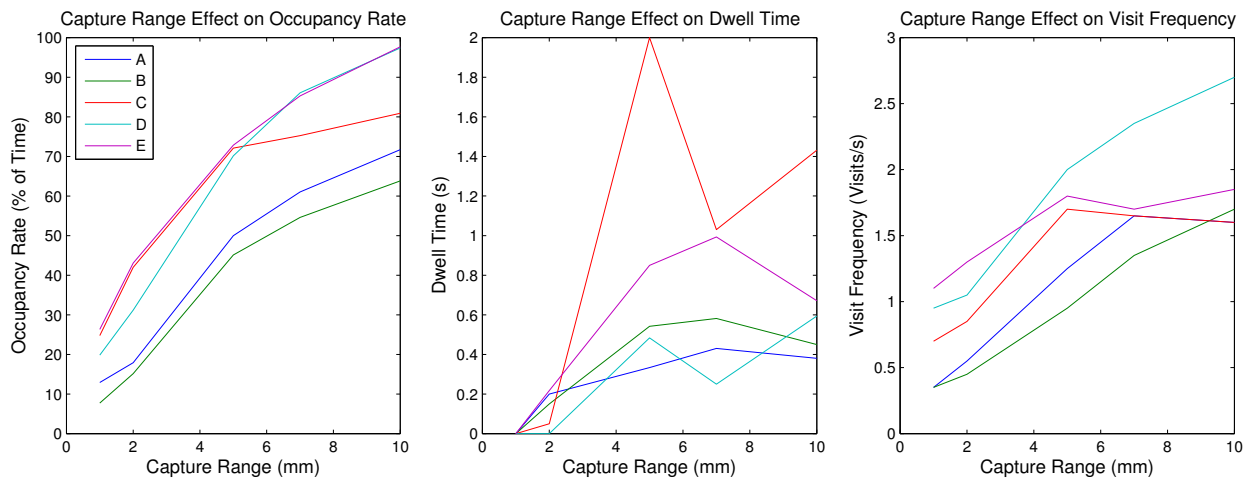


Figure 6. Effect of capture range on capture locations. Series A–E correspond to the datasets. Dwell time result C (*center*) is possible when the foreign body becomes trapped in a stationary part of the heart. A larger range leads to increased capture opportunity (e.g. greater perceived occupancy); of note is saturation at a range of roughly 7 mm.

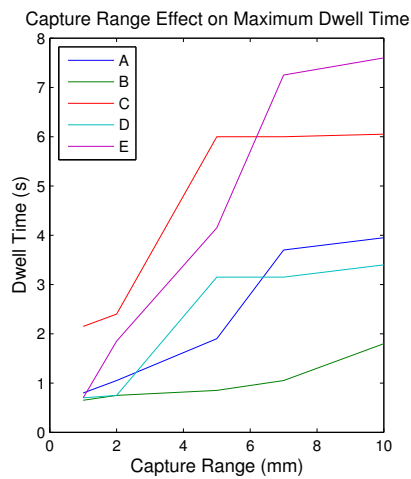


Figure 7. Effect of capture range on *maximum* dwell time (Fig. 6 [center] shows *average* dwell time.) The figures increase monotonically with capture range as expected, with saturation above 7 mm.

5. CONCLUSIONS

A minimally invasive surgical assistant for removal of foreign bodies from the heart has the potential to reduce health risks, mortality, perioperative time, and postoperative recovery time. Patients could return to normal activities sooner, and medical centers could treat more patients. Previously, the motion of a moving body in a beating heart phantom was quantified using motion tracking in 3D TEE images. We found the motion to be complex and difficult to predict in detail, and its speeds placed it beyond the capabilities of contemporary surgical robots. This observation gave rise to the notion of indirect pursuit to relax robot performance requirements.

We extended the concept of history-based location prediction to the identification of multiple candidate capture locations, based on spatial probability, dwell time, and visit frequency. First, the new information helps improve understanding of the motion, and can be incorporated into the design of an interventional system. Second, intraoperative selection from multiple candidates would allow for optimal effectiveness under constraints such as workspace, execution time, and reachability. The next milestones will involve the design of a robot control scheme that computes candidate capture locations in real time and selects the best retrieval path based on objective criteria. One important next step will be to determine how the presence of the robot affects the time spent in various locations. Studies of different numbers of moving bodies and physical properties are also important future tasks.

ACKNOWLEDGMENTS

Authors thank Emil Radulescu for insights on ultrasound technology, Douglas Stanton for assistance with the experimental setup, and Vijay Parthasarathy and Ameet Jain for assistance with the ultrasound equipment. This work was funded by Philips Research North America and Johns Hopkins University internal funds.

REFERENCES

- [1] United States Department of Defense, “Emergency War Surgery: Third United States Revision, s.l., 16: Thoracic Injuries,” (2004).
- [2] Williams, J. C. and Elkington, W. C., “Slow progressing cardiac complications—a case report,” *J. Chiropr. Med.* **7**, 28–33 (2008).
- [3] Symbas, P. N., Picone, A. L., Hatcher, C. R., and Vlasis-Hale, S. E., “Cardiac missiles. A review of the literature and personal experience.,” *Ann. Surg.* **211**, 639–47; discussion 647–8 (May 1990).
- [4] Marshall, A. J., Ring, N. J., and Newman, P. L., “An unexplained foreign body in the myocardium,” *J. Royal Soc. Med.* **95**, 250–251 (2002).
- [5] Actis Dato, G. M., Arslanian, A., Di Marzio, P., Filosso, P. L., and Ruffini, E., “Posttraumatic and iatrogenic foreign bodies in the heart: report of fourteen cases and review of the literature,” *J. Thorac. Cardiovasc. Surg.* **126**, 408–414 (Aug 2003).
- [6] Evans, J., Gray, L. A., Rayner, A., and Fulton, R. L., “Principles for the management of penetrating cardiac wounds,” *Ann. Surg.* **189**, 777–784 (Jun 1979).
- [7] Nessen, S. C. and Lounsbury, D. E., “War Surgery in Afghanistan and Iraq: A Series of Cases, 2003-2007, s.l. Department of the Army, Office of the Surgeon General and Borden Institute, 14: Thoracic Trauma,” (2008).
- [8] Steinhoff, J. P., Pattavina, C., and Renzi, R., “Puncture wound during CPR from sternotomy wires: case report and discussion of periresuscitation infection risks,” *Heart Lung* **30**, 159–160 (2001).
- [9] Krupa, A., Fichtinger, G., and Hager, G. D., “Real-time motion stabilization with B-mode ultrasound using image speckle information and visual servoing,” *Int. J. Robot. Res.* **28**(10), 1334–1354 (2009).
- [10] Stoll, J. A., Novotny, P. M., Howe, R. D., and Dupont, P. E., “Real-time 3D ultrasound-based servoing of a surgical instrument,” in [*IEEE Int. Conf. on Robotics and Automation*], 613–618 (2006).
- [11] Novotny, P. M., Stoll, J. A., Dupont, P. E., and Howe, R. D., “Real-time visual servoing of a robot using three-dimensional ultrasound,” in [*IEEE Int. Conf. on Robotics and Automation*], 2655–2660 (2007).
- [12] Whitman, J., Fronheiser, M. P., and Smith, S. W., “3-D ultrasound guidance of surgical robotics using catheter transducers: feasibility study,” *IEEE Trans. Ultrason., Ferroelectr., Freq. Control* **55**(5), 1143–5 (2008).

- [13] Yuen, S. G., Kettler, D. T., Novotny, P. M., Plowes, R. D., and Howe, R. D., “Robotic motion compensation for beating heart intracardiac surgery,” *Int. J. Robot. Res.* **28**(10), 1355–1372 (2009).
- [14] Kesner, S. B., Yuen, S. G., and Howe, R. D., “Ultrasound servoing of catheters for beating heart valve repair,” in [*Int. Conf. on Info. Proc. in Computer-Assisted Interventions*], *IPCAI’10*, 168–178, Springer-Verlag, Berlin, Heidelberg (2010).
- [15] Rogers, A. J., Light, E. D., and Smith, S. W., “3-D ultrasound guidance of autonomous robot for location of ferrous shrapnel,” *IEEE Trans. Ultrason., Ferroelectr., Freq. Control* **56**(7), 1301–3 (2009).
- [16] Fronheiser, M. P., Idriss, S. F., Wolf, P. D., and Smith, S. W., “Vibrating interventional device detection using real-time 3-D color Doppler,” *IEEE Trans. Ultrason., Ferroelectr., Freq. Control* **55**(6), 1355–62 (2008).
- [17] Liang, K., Allmen, D. V., Rogers, A. J., Light, E. D., and Smith, S. W., “Three-dimensional ultrasound guidance of autonomous robotic breast biopsy: feasibility study,” *Ultrasound Med. Biol.* **36**(1), 173–7 (2010).
- [18] Thienphrapa, P., Elhawary, H., Ramachandran, B., Stanton, D., and Popovic, A., “Tracking and characterization of fragments in a beating heart using 3D ultrasound for interventional guidance,” in [*Int. Conf. on Medical Image Computing and Computer-Assisted Intervention*], *MICCAI’11*, 211–218, Springer-Verlag, Berlin, Heidelberg (2011).
- [19] Ryan, K. L., Cooke, W. H., Rickards, C. A., Lurie, K. G., and Convertino, V. A., “Breathing through an inspiratory threshold device improves stroke volume during central hypovolemia in humans,” *J. Appl. Physiol.* **104**(5), 1402–9 (2008).
- [20] Novotny, P. M., Stoll, J. A., Vasilyev, N. V., del Nido, P. J., Dupont, P. E., Zickler, T. E., and Howe, R. D., “GPU-based real-time instrument tracking with three-dimensional ultrasound,” *Med. Image Anal.* **11**, 458–464 (2007).
- [21] Gonzalez, R. C. and Woods, R. E., [*Digital Image Processing*], Addison-Wesley Longman Publishing Co., Inc., Boston, MA, USA, 2nd ed. (2001).